Supporting information

Hybridization of preheated cellulose microcrystals with MoS_2 sheets for enhanced piezo-catalytic hydrogen evolution

Hailong Zhang,[a] Jianzhong Guo,[a] Shuying Liang,[a] Hongbo Yu,*[b] Xianhong Li *[c] and Chunzheng Wu *[a] [a] *Zhejiang Key Laboratory of Green and Low-Carbon Utilization Technology of Agricultural and Forestry Biomass, College of Chemistry and Materials Engineering, Zhejiang A&F University, Hangzhou 311300, P. R. China.*

[b] *School of Materials and Chemical Engineering, Ningbo University of Technology, Ningbo 315211, P. R. China*

[c] *Hangzhou Lin'an Huier Molybdenum Industry Science & Technology Co., Ltd., Hangzhou 311300, P. R. China.*

* Corresponding authors: hongboyu@nbut.edu.cn (H. Yu), lixh6999@163.com (X. Li), wucz@zafu.edu.cn (C. Wu)

Experimental section

1. Chemicals

Microcrystalline cellulose (97%) and thiourea (CH_4N_2S, ≥ 98.0%) were purchased from MREDA. Ammonium heptamolybdate tetrahydrate ($(NH_4)_6Mo_7O_{24}\cdot 4H_2O$, AR), glucose ($C_6H_{12}O_6$, AR), ethanol ($C_2H_6O$, AR), chloroplatinic acid hexahydrate ($H_2PtCl_6\cdot 6H_2O$, AR), methanol (CH_4O, AR), sodium sulfide (Na_2S, ≥97%), ascorbic acid ($C_6H_8O_6$, AR), and lactic acid ($C_3H_6O_3$, AR) were obtained from Sinopharm Group. Triethanolamine ($C_6H_{15}NO_3$) was purchased from Aladdin. Sodium sulfite (Na_2SO_3, ≥98%) was purchased from DAMAS.

2. Preparations

Preheated microcrystalline cellulose (CL): Microcrystalline cellulose (2 g, 97%, MREDA) was placed in a covered crucible and heated in a muffle furnace to 350 °C at a ramp rate of 5 °C min^{-1}. The temperature was maintained for 2 h to partially carbonize the surface, yielding the preheated cellulose (CL).

CL@MoS_2 heterostructures: 1.24 g of ammonium molybdate tetrahydrate ($(NH_4)_6Mo_7O_{24}\cdot 4H_2O$), 2.208 g of thiourea ($CS(NH_2)_2$, ≥99.0%), and 0.15 g of CL were sequentially added to 35 mL of deionized water under ultrasonic agitation for 10 min to form a homogeneous suspension. The mixture was then transferred into a Teflon-lined stainless-steel autoclave and subjected to a hydrothermal reaction at 180 °C for 24 h. After cooling to room temperature, the resulting black precipitate was collected, washed three times with deionized water, and dried at 70 °C in a vacuum oven for 12 h. The obtained CL@MoS_2 composite contained 59.2 wt.% MoS_2 and, unless otherwise specified, is referred to as "CL@MoS_2" throughout this work. To tune the MoS_2 loading from 36.3 wt.% to 72.2 wt.%, the amount of CL was varied from 1.2 g to 0.05 g while maintaining all other synthesis parameters constant.

3. Characterizations

X-ray diffraction (XRD) measurements were carried out on a Shimadzu Lab XRD-6100 diffractometer using Cu Kα radiation (λ = 0.1541 nm). N_2 adsorption-desorption isotherms were recorded at 77 K using an ASAP2460 analyzer. X-ray photoelectron spectroscopy (XPS) was performed on a Shimadzu/Kratos AXIS SUPRA+ system. Inductively coupled plasma optical emission spectroscopy (ICP-OES) was conducted with an Avio 220 Max. For these measurements,

MoS_2-containing samples were digested in aqua regia under heating for 4 hours and subsequently filtered to determine the Mo concentration. The MoS_2 loading was calculated assuming that all detected Mo existed in the form of MoS_2. Piezoelectric force microscopy (PFM) was carried out using a Bruker Dimension Icon.

4. Electrochemical test

Electrochemical measurements were conducted using a CHI660E workstation equipped with a standard three-electrode configuration in 0.5 M Na_2SO_4 electrolyte. A platinum wire served as the counter electrode, and a saturated Ag/AgCl electrode was used as the reference. The working electrode was fabricated by dispersing 10 mg of catalyst in 5 mL ethanol containing 80 μL of 5 wt.% Nafion solution, followed by 30 min of ultrasonication. Then, 10 μL of the resulting ink was drop-cast onto a pre-cleaned FTO glass substrate (1×1 cm^2) and dried at 80 ^oC for 2 h. Piezoelectric current responses were measured by immersing the electrochemical cell in a 160 W ultrasonic bath, recording the i-t curves under periodic on/off cycles. Electrochemical impedance spectroscopy (EIS) was performed at an overpotential of 600 mV in the frequency range of 0.01 Hz to 100 kHz using a 5 mV AC perturbation. Polarization curves for H_2 evolution were recorded by linear sweep voltammetry (LSV) at 5 $mV \cdot s^{-1}$.

5. Piezocatalytic tests

A total of 10 mg of catalyst powder was dispersed in 20 mL of glucose solution (2.8 $molL^{-1}$) in a 60 mL glass reactor. An appropriate amount of H_2PtCl_6 solution was then added to achieve a Pt loading of 2 wt.% on the catalyst. The suspension was purged with high-purity argon (99.999 %) for 30 min to remove dissolved oxygen and subsequently sealed with a silicone rubber septum. The reactor was irradiated under a 365 nm UV LED lamp with continuous stirring for 1 h. Afterward, the stirring bar was removed, and the reactor was purged again with pure Ar. The reactor was then placed at the center of an ultrasonic bath operating at 40 kHz and 160 W. To prevent excessive heating, the bath water was refreshed every 15 min to maintain the temperature below 30 ^oC. Gas samples (100 μL) were collected hourly using a gas-tight syringe and analyzed for hydrogen content with a gas chromatograph (s·sun GC-9860) equipped with a thermal conductivity detector (TCD).

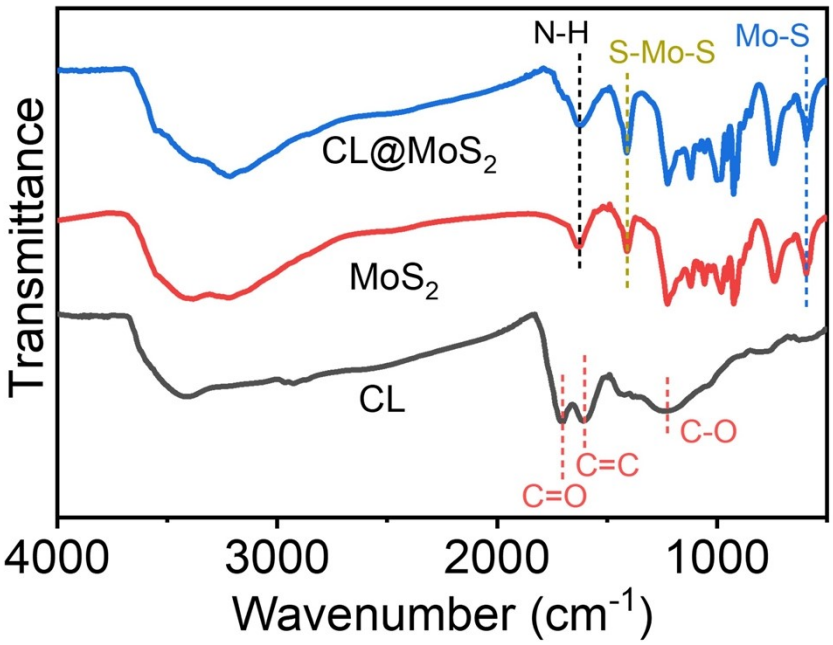

Fig.S1 FTIR spectra of CL, MoS_2 and CL@MoS_2. For CL, characteristic peaks appear at 1707, 1601, and 1226 cm^{-1}, corresponding to C=O stretching[1], aromatic C=C stretching[2], and C-O stretching[3], respectively. MoS_2 and CL@MoS_2 show similar FTIR features, with a peak at 594 cm^{-1} attributed to Mo-S stretching, a peak at 1408 cm^{-1} assigned to S-Mo-S stretching[4], and a band at 1633 cm^{-1} arising from N-H bending[5]. Additional peaks between 730-1250 cm^{-1} possibly originate from the decomposition products of Mo and S precursors and are difficult to assign unambiguously.

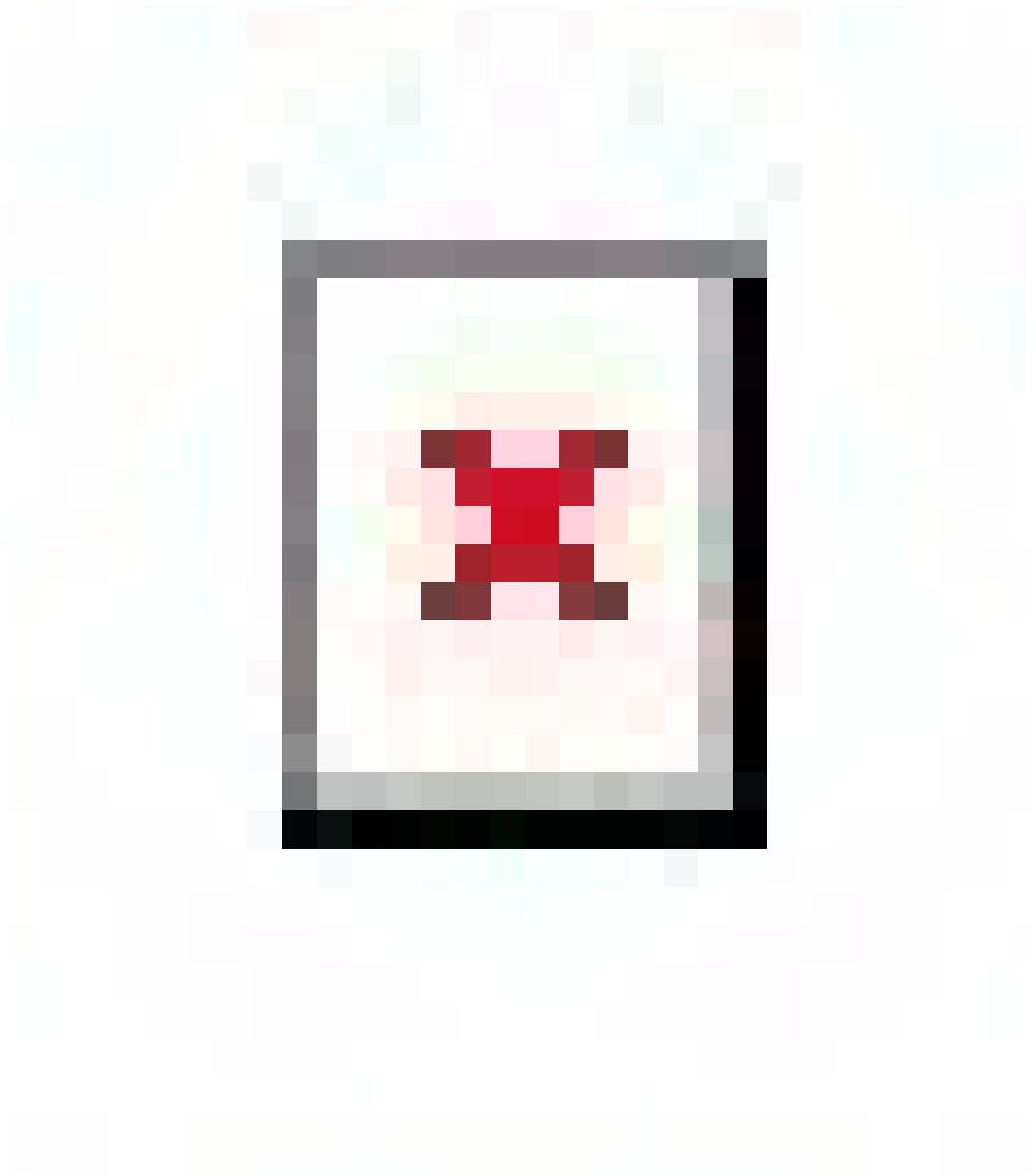

Fig.S2 Influence of (a) different metal cocatalysts (2 wt.%), (b) Pt loading amounts, (c) glucose solution pH, (d) glucose concentration, and (e-f) catalyst dosage on the H_2 evolution performance of CL@MoS_2.

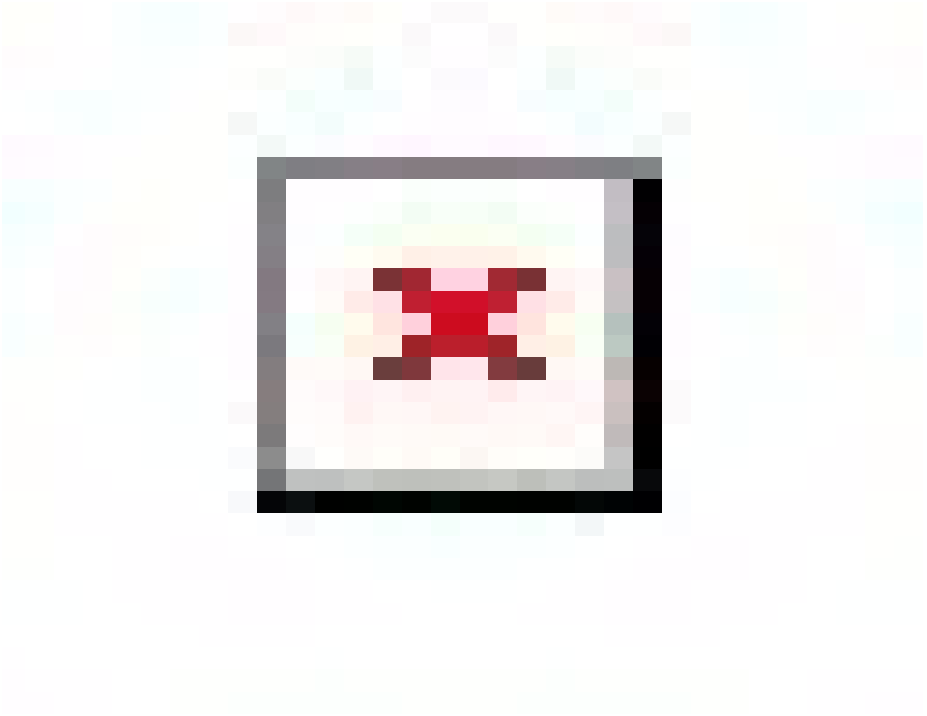

Fig.S3 (a, b) SEM images and (c, d) corresponding EDS elemental mappings of the CL@MoS_2 sample containing 72.2 wt.% MoS_2, showing that individual MoS_2 microflowers have grown independently from the CL surface.

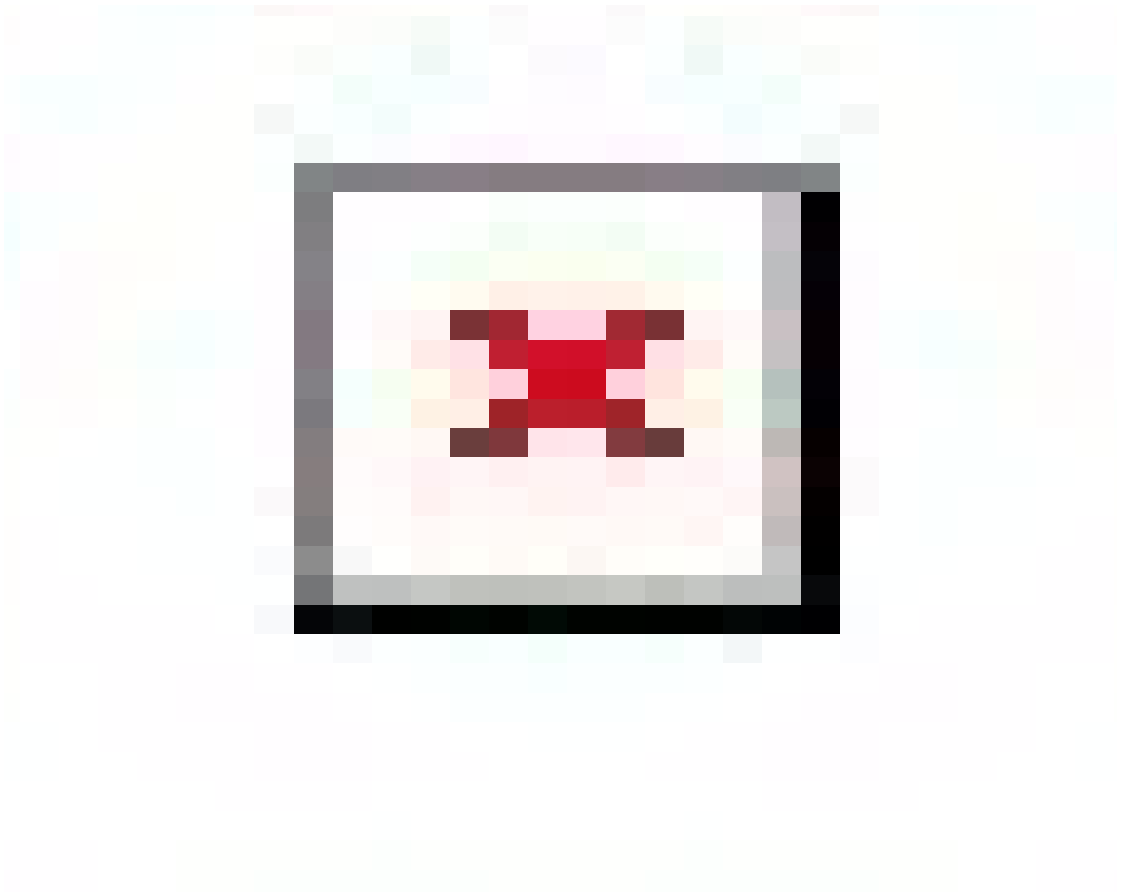

Fig.S4 (a) XRD patterns and (b) FTIR spectra of CL@MoS_2 before and after the recyclability tests; (b) SEM image and corresponding EDS elemental mappings of CL@MoS_2 following the recyclability tests. For FTIR, a clear decrease in the intensities of the Mo-S and S-Mo-S vibration bands is observed, indicating partial surface oxidation of MoS_2 during long-term operation. This minor oxidation does not affect the long-range bulk crystallinity, as shown by XRD. In addition, most peaks in the 730-1250 cm^{-1} region disappear after the reaction, likely due to the removal of residual organic groups (originating from the Mo and S precursors) from the MoS_2 surface during the piezocatalytic test under sonication.

Table S1. A comparison of our CL@MoS_2 catalyst with the reported piezocatalysts in H_2 evolution.

Photocatalyst	HER rate (mmol/g/h)	Sonication	Conditions	Reference
CL@MoS_2	~1.0	40 kHz, 160 W	10 mg / 20 mL Pure water	This work
	2.96	40 kHz, 160 W	10 mg / 20 mL 2.8 M Glucose	This work
	~7	40 kHz, 160 W	10 mg / 20 mL 10 % Methanol	This work
UT g-C_3N_4	8.35	40 kHz, 240 W	2 mg / 100 mL 0.1 M Glucose	Hu et al. [6]
2D Te	9	53 kHz, 100 W	5 mg/100 mL 15 % TEOA	Mishra et al. [7]
CdS/BiOCl	1.05	40 kHz, 120 W	50 mg / 20 mL 20 % Methanol	Hao et al. [8]
Bi_{8h}/BiOCl	2.81	40 kHz, 160 W	10 mg / 20 mL 1.4 M Glucose	Su et al. [9]
BiOCl	0.98	40 kHz, 120 W	5 mg / 5 mL 2 % Methanol	Long et al. [10]
$Bi_2Fe_4O_9$ nanoplates	5.72	40 kHz, 200 W	2 mg / 10 mL 10 % Methanol	Du et al. [11]
Hollow $CaTiO_3$ Nanocuboids	3.44	40 kHz, 250 W	2 mg / 10 mL 10 % Methanol	Zhou et al. [12]
CN-$C_{0.025}$	3.92	40 kHz, 160 W	10 mg / 20 mL 10 % Methanol	Nie et al. [13]
$ZnSnO_3$ nanowires	3.45	40 kHz, 250 W	10 mg / 10 mL 50 % Methanol	Wang et al. [14]
MIL-100(Fe)	2.8	40 kHz, 120 W	5 mg / 5 mL 1 % Methanol	He et al. [15]
MoS_2@Mo_2CT_x	1.16	40 kHz, 250 W	10 mg / 10 mL 25 % Methanol	Lin et al. [16]

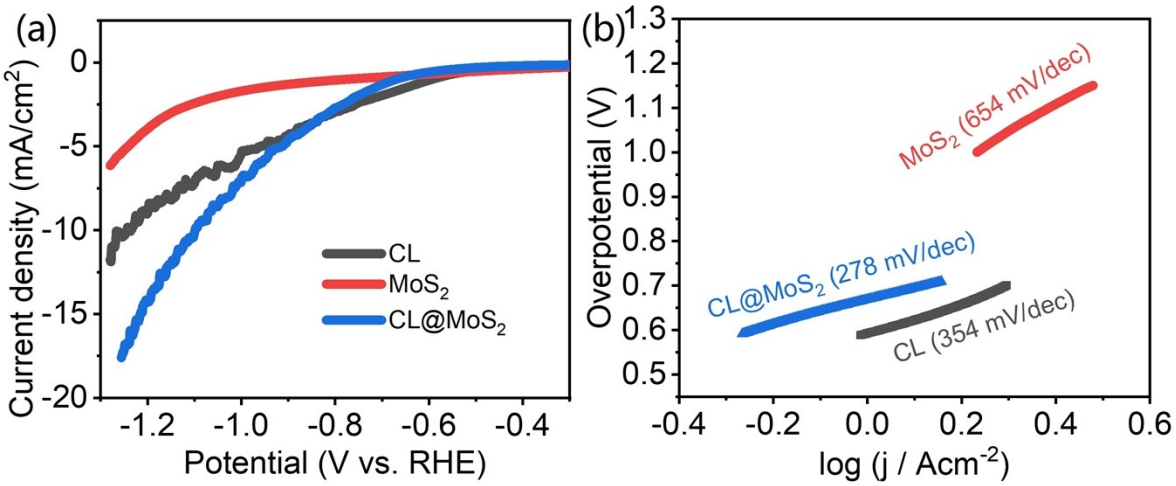

Fig.S5 (a) LSVs and the corresponding (b) Tafel plots of CL, MoS_2 and CL@MoS_2. Notably, MoS_2—despite being a well-known HER catalyst—shows the lowest activity in this system, which may be attributed to factors such as material assembly, active-site exposure, or surface water affinity.

Fig.S6 Water contact angles of (a) CL, (b) MoS_2 and (c) CL@MoS_2. Both CL and MoS_2 are hydrophobic, while the CL@MoS_2 heterostructure shows a much lower contact angle of 58°, indicating markedly enhanced hydrophilicity. The underlying cause of this unexpected behavior is unclear but may be related to changes in surface morphology or the presence of surface defects.

Reference

1. E. Fumoto, S. Sato, Y. Kawamata, Y. Koyama, T. Yoshikawa, Y. Nakasaka, T. Tago and T. Masuda, *Fuel*, 2022, **318**, 123530.
2. M. K. Trivedi, S. Patil, H. Shettigar, K. Bairwa and S. Jana, *Medicinal Chemistry*, 2015, **5**, 340-344.
3. B. Mohebby, *Journal of Agricultural Science and Technology*, 2010, **10**, 253-259.
4. M. E. M. Ali, R. Mohammed, S. M. Abdel-Moniem, M. A. El-Liethy and H. S. Ibrahim, *Journal of Nanoparticle Research*, 2022, **24**, 191.
5. Y. Jiang, Y. Li, C. Richard, D. Scherman and Y. Liu, *Journal of Materials Chemistry B*, 2019, **7**, 3796-3803.
6. C. Hu, F. Chen, Y. Wang, N. Tian, T. Ma, Y. Zhang and H. Huang, *Advanced Materials*, 2021, **33**, 2101751.
7. H. K. Mishra, Ankush, N. Barman, B. Mondal, M. Jha, R. Thapa and D. Mandal, *Small*, 2024, **20**, 2402421.
8. P. Hao, Y. Cao, X. Ning, R. Chen, J. Xie, J. Hu, Z. Lu and A. Hao, *Journal of Colloid and Interface Science*, 2023, **639**, 343-354.
9. F. Su, J. Nie, H. Yu, S. Yue, J. Guo and C. Wu, *Inorganic Chemistry*, 2025, **64**, 9195-9203.
10. Y. Long, H. Xu, J. He, C. Li and M. Zhu, *Surfaces and Interfaces*, 2022, **31**, 102056.
11. Y. Du, T. Lu, X. Li, Y. Liu, W. Sun, S. Zhang and Z. Cheng, *Nano Energy*, 2022, **104**, 107919.
12. H. Zhou, J. Cao, Y. Ji, M. Xia and W. Yao, *Small*, 2024, **20**, 2402679.
13. J. Nie, S. Yue, B. Li, J. Guo and C. Wu, *Ceramics International*, 2025, **51**, 31370-31377.
14. Y.-C. Wang and J. M. Wu, *Advanced Functional Materials*, 2020, **30**, 1907619.
15. J. He, Z. Yi, Q. Chen, Z. Li, J. Hu and M. Zhu, *Chemical Communications*, 2022, **58**, 10723-10726.
16. H.-Y. Lin and J. M. Wu, *Advanced Energy Materials*, 2024, **14**, 2402164.